Reactions between Triazolinediones and Equilibrating Forms of Cycloheptatriene Derivatives Featuring 7,7-Spiro and 1,7-Fused Heterocyclic Rings

Mauro Freccero,[a] Remo Gandolfi,*[a] Mirko Sarzi-Amade',[a] and Bruna Bovio[b]

Keywords: Cycloadditions / Cycloheptatriene derivatives / Density functional calculations / Nitrogen heterocycles

Nitrile oxide–azaheptafulvene adducts consist of rapidly equilibrating mixtures of fused (**1**) and spiro (**2**) isomers, the relative stabilities of which are nicely reproduced by B3LYP/6-31G* calculations. The reaction between these compounds and MTAD affords only two diastereomeric adducts [**9** (dominant) and **10**], both deriving from the reaction of MTAD with **1** even in cases in which that isomer could not be detected by NMR spectroscopy. These adducts are formal Diels–Alder adducts deriving from attacks on the two diastereotopic faces of the triene moiety of **1** and involving only the diene system adjacent to the amino substituent (N^4–C^{4a}=C^5–C^6=C^7). The structures of the adducts are firmly supported by spectroscopic data and X-ray analysis, and so previous incorrect assignments are revised. The mechanism of the reaction between MTAD and **1** is briefly discussed.

Introduction

We have shown[1,2] that the attack by aromatic and aliphatic nitrile oxides on azaheptafulvenes (cycloheptatriene-1-imines) always takes place either exclusively or preferentially at the C=N double bond moiety, to afford a rapidly equilibrating mixture (NMR analysis) of the 1,7-disubstituted cycloheptatriene isomers (the 4,9a-dihydrocyclohepta-1,2,4-oxadiazine derivatives **1***cht*[3]) and the 7,7-disubstituted derivatives (the 1,2,4-oxadiazaspiro[4.6]undeca-2,6,8,10-tetraene derivatives **2***cht*), the ratio of which strongly depends on R^1 (Scheme 1, Table 1).

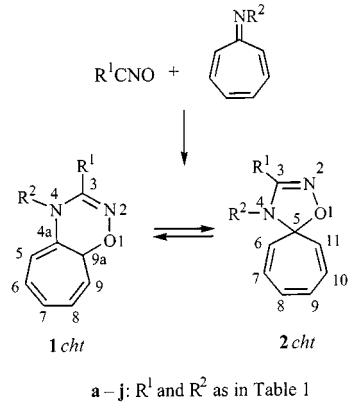

Scheme 1

Table 1. Ratios (%) between the "fused" (**1***cht*) and the "spiro" (**2***cht*) isomers in C_6D_6 and CD_3CN at 20 °C

Compd.[a]	R^1	R^2	C_6D_6 **1/2**	CD_3CN **1/2**
a	*t*Bu	*p*-tolyl	0:100	
b	Ph	*p*-tolyl	8:92	
c	Me	*p*-tolyl	70:30	42:58
d	Me	Me	90:10	53:47
e	2,6-$Cl_2C_6H_3$	Me	94:6	88:12
f	MeCO	*p*-tolyl	41:59[b]	
g	PhCO	*p*-tolyl	52:48[c]	
h	2,4,6-$Me_3C_6H_2$	*p*-tolyl	46:54	31:69
i	2,4,6-Me_3-3,5-Cl_2C_6	*p*-tolyl	76:24	48:52
j	2,6-$Cl_2C_6H_3$	*p*-tolyl	92:8	75:25

[a] Ratios in $CDCl_3$ are, as a rule, similar to those in C_6D_6. [b] In C_7D_8 at − 40 °C. [c] In CD_2Cl_2 at − 50 °C.

Saito et al. also investigated the same reaction (using *p*-substituted benzonitrile oxides), but only the dominant spiro isomer **2** was detected by them.[4,5] Moreover, they discussed[5] the (possible) equilibrium between the cycloheptatriene derivatives **2***cht* and their norcaradiene isomers **2***ncd* while overlooking the possible 1,7-sigmatropic shift of oxygen or nitrogen to give a condensed isomer of type **1***cht* (and consequently also its norcaradiene isomer **1***ncd*). Actually, only the 1,7-oxygen shift occurs, to give **1***cht* from **2***cht* and vice versa, most probably through a dipolar intermediate (see Scheme 2, in which the equilibria for compounds **d** are reported).

[a] Dipartimento di Chimica Organica,
Viale Taramelli 10, 27100 Pavia, Italy
E-mail: gandolfi@chifis.unipv.it
[b] Dipartimento di Chimica Generale,
Viale Taramelli 12, 27100 Pavia, Italy
Supporting information for this article is available on the WWW under http://www.eurjoc.com or from the author.

  1434−193X/02/0203−0569 $ 17.50+.50/0

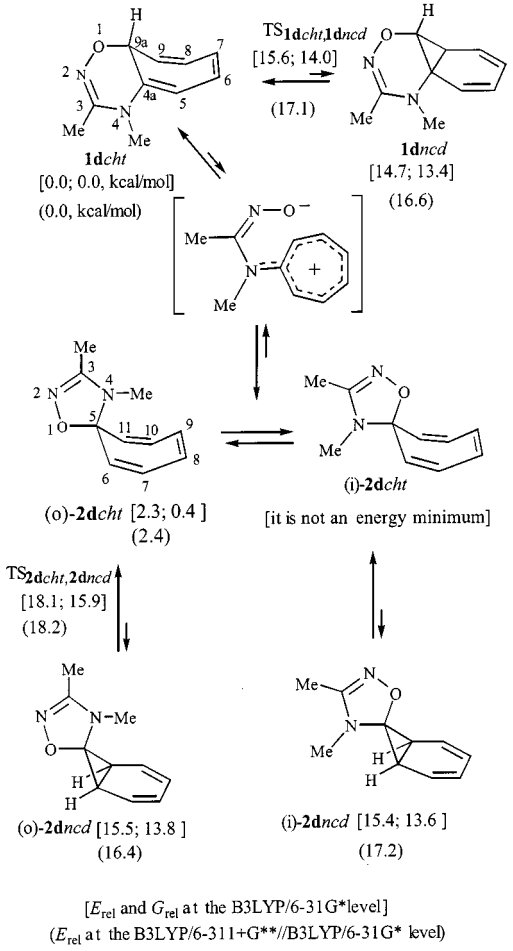

Scheme 2

As for chemical reactions of nitrile oxide−azaheptafulvene adducts, catalytic hydrogenation afforded only products derived from the spiro form **2***cht* no matter which side the **1***cht*/**2***cht* equilibrium was shifted towards. Thermal decomposition of **1***cht*/**2***cht* produced benzene, R^1CN, and R^2NCO, strongly suggesting that the undetectable (by spectroscopic techniques) isomer **2***ncd* (Scheme 2) was an intermediate on the pathway to these products.[1,2]

The most obvious way to trap norcaradiene isomers (**1***ncd* and **2***ncd*) consists of a Diels−Alder reaction with a reactive dienophile such as a 1,2,4-triazoline-3,5-dione [TAD, *N*-methylTAD (MTAD), or *N*-phenylTAD (PTAD)].[6−12] In fact, in their reaction with TADs, not only the parent cycloheptatriene **3a***cht* but also, for example, the spiro compound **3e***cht*[9] (Scheme 3) and a derivative of **4***cht* (Scheme 4) (**7**; Scheme 5)[10] have been reported to produce only the Diels−Alder adducts (**6a**, **6e**, and **8**; Scheme 5) derived from the undetectable norcaradiene isomer.

In the case of nitrile oxide−azaheptafulvene adducts **1**/**2**, there are several equilibrating isomers (see Scheme 2 for compounds **d**) that can compete with each other to give Diels−Alder adducts (see Scheme 6, bottom).[13] The reactivity of norcaradiene isomers should be enhanced by planarity in their diene moieties, while the triene system in **1***cht* (i.e., both $C^{4a}-C^5-C^6-C^7$ and $C^6-C^7-C^8-C^9$ dienes) is certainly activated by the electron-donating effect of the amino substituent.

Saito et al. reported that the reaction (in dichloromethane at room temperature) between arylnitrile oxide−azaheptafulvene adducts (such as **1b/2b**, R^1 = Ph and R^2 = *p*-tolyl) and *N*-phenyltriazolinedione (PTAD) was completely chemo- and diastereoselective.[5] They claimed the isolation, in fair to good yields, exclusively of adducts derived from the attack of PTAD on the spiro isomer **2***cht*, at the face *syn* to the oxadiazoline ring oxygen atom (namely adducts of type **13**, such as **13k** in Scheme 6). This result must be revised. In fact, we have shown that triazolinediones react very readily with nitrile oxide−azaheptafulvene adducts to afford high yields of mixtures of two facial diastereoisomeric adducts [namely, **9** and **10** (Scheme 6), with **9** strongly predominating] derived from the reaction between TAD and the $C^{4a}-C^5-C^6-C^7$ diene moiety of the fused isomer **1***cht*.

Results

Reactant Structures

The equilibrium ratios for derivatives **1/2**, the reactions of which with MTAD are described in this paper, are reported in Table 1. These derivatives were chosen because they span the range from complete or pronounced dominance of the "spiro" form **2***cht* (Entries **a** and **b** in Table 1) to strong prevalence of the "fused" form **1***cht* (Entries **d**, **e**, and **j**). Moreover, in this series there are derivatives in which the **1/2** equilibrium is fast enough to give rise to averaged ^{1}H NMR spectra even at room temperature (Entries **f** and **g**, R^1 = MeCO and PhCO, R^2 = *p*-tolyl) and derivatives (**a**−**e** and **h**−**j**) the equilibria of which are slow on the NMR timescale, so that well-resolved signals for both components are seen in spectra recorded at room temperature.[1,2]

As far as we know, derivatives **1/2** represent the only examples in which a 7,7-cycloheptatriene derivative equilibrates rapidly with its 1,7-counterpart with both isomers present in significant amounts (that is, both are detectable by NMR spectroscopy).[14−19]

In order to find out whether there is some relationship between the product outcome of the reaction with TADs and the relative energies and geometrical structures of isomers of nitrile oxide−azaheptafulvene adducts, we carried out DFT calculations with the hybrid B3LYP/6-31G* method for derivatives **1d/2d** (R^1 = R^2 = Me). The relative potential energies {both at the B3LYP/6-31G* [E_{rel}, kcal/mol] and B3LYP/6-311+G**//B3LYP/6-31G* levels (E_{rel}, kcal/mol)} and free energies {at the B3LYP/6-31G* level [G_{rel}, kcal/mol]} for all the possible equilibrating isomers [and some of the transition structures (TSs) involved in their interconversion] are reported in Scheme 2. Schemes 3 and 4 give collected computational data for related cyclo-

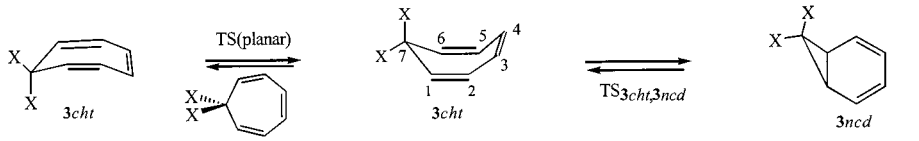

a: X = H	[5.2; 5.4] (5.5)	[0.0; 0.0] (0.0)	[9.9; 9.6] (10.7)	[6.5; 6.8] (8.1)
b: X = F	[0.5; 0.5] (–0.1)	[0.0; 0.0] (0.0)	[15.6; 15.4] (16.8)	[14.9.; 15.1] (16.7)
c: X = CN	[4.9; 5.7] (5.2)	[0.0; 0.0] (0.0)	[7.8; 7.6] (8.3)	[-3.1; -2.3] (-1.4)
d: X–X = $O(CH_2)_2O$	[0.1; 0.5] (0.3)	[0.0; 0.0] (0.0)	[13.4; 12.4] (13.8)	[12.0; 12.5] (13.1)
e: X–X = $O(CH_2)_3O$	[3.8; 2.7] (3.8)	[0.0; 0.0] (0.0)	[9.7; 9.1] (10.3)	[7.1; 7.4] (8.5)

[E_{rel} and G_{rel}, kcal/mol, at the B3LYP/631G* level]
(E_{rel}, kcal/mol, at the B3LYP/6-311+G**//B3LYP/6-31G* level)

Scheme 3

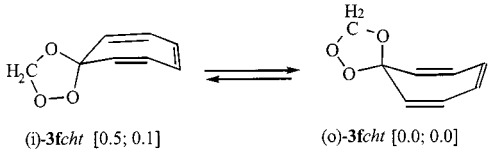

[E_{rel} and G_{rel}, kcal/mol, at the B3LYP/6-31G* level]
(E_{rel}, kcal/mol, at the B3LYP/6-311+G**//B3LYP/6-31G* level)

Scheme 4

heptatriene derivatives, the reactions of which with TADs (Scheme 5) have already been studied.[8,9]

It is well known that cycloheptatriene and its 7,7-derivatives (such as **3a***cht*–**3e***cht*, Scheme 3) adopt boat conformations[6,20–22] and that the α, β, and γ angle values (Figure 1; quite different from 0°; Table 2) for these compounds provide support for this view. However, the potential energy surface related to the ring inversion is, as a rule, quite flat, and the planar TS can reside less than 0.5 kcal higher than the two equivalent interconverting boat structures, as in the cases of the 7,7-difluorocycloheptatriene **3b***cht* and the 7,7-ethylenedioxycycloheptatriene **3d***cht* (Scheme 3).

These last two examples demonstrate that the energy necessary to planarize the cycloheptatriene ring can be very low even when the ground-state structure features a pronounced concave array of atoms (Table 2). Recently, an example of planarization of the seven-membered ring in the ground state has been reported; the cycloheptatriene ring in

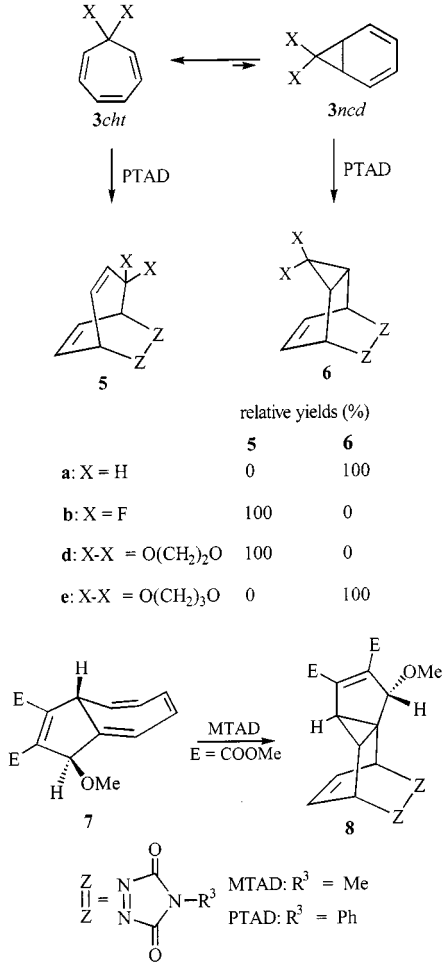

relative yields (%)

	5	**6**
a: X = H	0	100
b: X = F	100	0
d: X-X = $O(CH_2)_2O$	100	0
e: X-X = $O(CH_2)_3O$	0	100

Scheme 5

spiro ozonide **3f***cht* in Scheme 4 has been found to be planar (B3LYP/6-31G* calculations) in its ground state and this observation has been explained in terms of "the formation of a structure with partial tropylium ion character".[23]

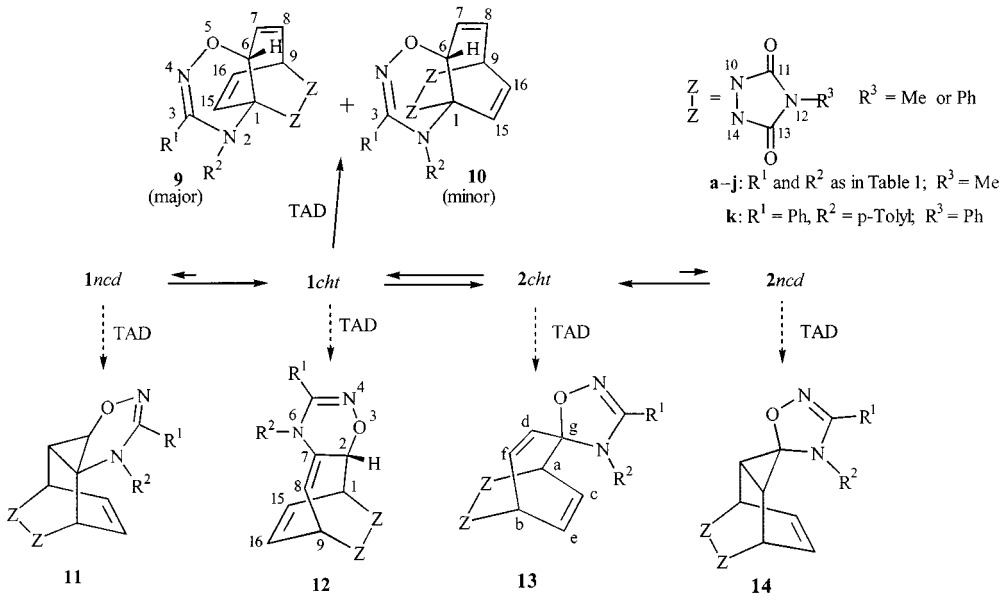

Scheme 6

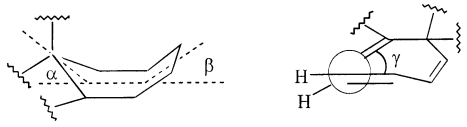

Figure 1. Dihedral angles (α, β, and γ used to describe nonplanarity of the cycloheptatriene moiety in compounds **1***cht*−**4***cht*

Table 2. Geometrical data (angles α, β, and γ in °; Figure 1) for cycloheptatriene derivatives **1***cht*−**4***cht*

	α	β	γ[a]
1d*cht*	59.5	24.5	29.0
(o)-**2d***cht*	30.5	13.0	16.5
3a*cht*	53.0	25.0	30.5
3b*cht*	39.7	16.2	20.3
3c*cht*	50.5	23.5	29.2
3d*cht*	39.6	16.8	21.1
3e*cht*	47.9	20.7	25.6
(i)-**3f***cht*	33.5	14.1	17.9
(o)-**3f***cht*	6.9	2.8	3.6
4*cht*	51.4	24.1	29.3

[a] The torsional angles γ for the two diene systems of the cycloheptatriene moiety are either equal or very similar to each other (the average absolute value is reported).

We could not fully reproduce this result, as we found two minima [(i)-**3f***cht* and (o)-**3f***cht*],[24] which were, however, very similar to each other as far as energy was concerned, and in which the cycloheptatriene moiety of the more stable structure [(o)-**3f***cht*] was actually very close to planarity, thus substantially confirming previous calculations and the flatness of the ring-inversion potential-energy surface for these systems. In fact, the behavior of **3f***cht* is not an exception, but it is similar to that of **3b***cht* and **3d***cht* and all these derivatives exhibit high planar-boat flexibility.

We feel that a planar structure is also favored for **3b***cht*, **3d***cht*, and **3f***cht*, as well as by a possible tropylium ion character,[25] by the fact that it minimizes the repulsion between the high electron density on the oxygen or fluorine atoms at position 7 and the cycloheptatriene π-bond system. This observation is consistent with the finding that, in the case of compound **2d***cht*, the NMe moiety prefers to reside inside the cycloheptatriene "tub" (Scheme 2) despite its larger steric demand in comparison to the oxygen atom. In fact, (o)-**2d***cht* ($R^1 = R^2 = Me$) is more stable than (i)-**2d***cht* (the latter structure[26] does not in fact correspond to an energy minimum at the B3LYP/6-31G* level); the positively charged methyl group shields the negative nitrogen atom in the former structure, making electrostatic interactions of the NMe group with the π-system more favorable than those involving the oxygen atom.[26]

It is important to underline the fact that the energy necessary to force compound **2d***cht* from the (o) conformation to a planar form is low (0.6 kcal/mol evaluated from a constrained optimization), which is consistent with what has been observed for **3b***cht* and **3d***cht*. All these compounds can easily adopt a planar conformation if this is required by the reaction they are involved in.

Finally, it is interesting to note that the planarizing effect of oxygen atoms at position 7 is definitely higher when they are incorporated in a five-membered ring (as in **3d***cht*) than it is when they are part of a six-membered ring (as in **3e***cht*), as can clearly be inferred from geometrical parameters (Table 2) and from activation energies for ring-inversion (Scheme 3).

In 1,7-fused cycloheptatrienes **1***cht* and **4***cht*, the seven-membered ring inversion is no longer an easy process, and calculations indicate that only conformers with the bridgehead hydrogen atom pointing inside [such as **1d***cht* (Scheme 2) and **4***cht* (Scheme 4)] are energy minima. The

energies necessary to force the triene systems of **1***cht* and **4***cht* into planar structures are relatively large, 8.3 and 7.0 kcal/mol, respectively.

The (i) and (o)[3] conformers of **2***cht* can cyclotautomerize to give the spiro norcaradiene derivatives (i)-**2***ncd* and (o)-**2***ncd*, respectively, the energies of which are much higher (by > 13 kcal/mol) than those of their cycloheptatriene counterparts (Scheme 2). This behavior is consistent with the well-known observation that cycloheptatriene substituents, that can act as σ-acceptor and π-donor (as the oxygen and NMe group in compounds **2**) at position 7, heavily shift the cycloheptatriene/norcaradiene equilibrium to the left by destabilizing the norcaradiene isomer.[20] This observation is also clearly borne out by the computational results obtained for the 7,7-difluoro (**3b**) and 7,7-ethylenedioxy (**3d**) derivatives (Scheme 3), with the *ncd* isomers residing at higher energies (by > 12 kcal/mol) than the corresponding *cht* derivative. Also interesting is the observation that the strongly destabilized norcaradiene isomers (**1***ncd*, **3b***ncd*, **3d***ncd*) reside in very flat potential energy wells and that **3d***ncd* no longer seems to be a minimum if free energy is considered. Here, again, the effect of oxygen atoms in enhancing the energies of the *ncd* isomers almost completely disappears in the case of a six-membered ring; **3e***ncd* is 7 kcal/mol higher in energy than **3e***cht*, a gap not significantly different from the 6.5 kcal/mol difference calculated for the parent system (**3a***cht*/**3a***ncd*).

Finally, it should be observed that the presence of a 1,7-fused ring does not particularly disfavor the norcaradiene structure. In fact, fused **1d***ncd* has a stability similar to that of spiro **2d***ncd* (Scheme 2) and the increase in energy on going from **4***cht* to **4***ncd* (Scheme 4) is similar to that on passing from **3a***cht* to **3a***ncd* (Scheme 3).

As to the reliability of the method used, the B3LYP/6-31G* calculations[27] acceptably reproduce the experimentally observed dominance of **1d***cht* over **2d***cht* [ΔG(benzene) = 1.30 kcal/mol; Table 1][28] and of cycloheptatriene (**3a***cht*) over norcaradiene (**3a***ncd*) ($\Delta G \approx 4$ kcal/mol),[29] the reversal of stability of the two valence tautomers in the case of 7,7-dicyano substitution (**3c***ncd* more stable than **3a***cht*; $\Delta G > 4$ kcal/mol),[30] the activation energy of ring inversion of cycloheptatriene (6.3 kcal/mol)[31] and the activation free energy of cyclization of cycloheptatriene to norcaradiene (ca. 11 kcal/mol).[32]

It is noteworthy that energy refinement (in parentheses in Schemes 3 and 4) by single-point calculations with a significantly larger basis set (i.e., on passing from B3LYP/6-31G* to B3LYP/6-311+G**//B3LYP/6-31G*) substantially confirms all the observations based on B3LYP/6-31G* data. Actually, the larger basis set data seem to be poorer with respect to experimental data, apparently as a consequence of overestimation of angle strain destabilization of norcaradiene derivatives. It might be that also B3LYP/6-31G* data are slightly flawed by this drawback.

Reactions between 1/2 and MTAD

The reactions between compounds **1/2** and MTAD took place so readily at room temperature that they looked like titrations. In fact, when a red benzene solution of freshly sublimed MTAD was added dropwise to a benzene solution of **1/2**, the red color disappeared rapidly (from a few seconds to a few minutes) and the end of the reaction was clearly indicated by color persistence. Evaporation of the solvent gave almost quantitative yields of a product that consisted (NMR and TLC analysis) either of a pure Diels–Alder adduct or of a mixture of two Diels–Alder adducts. When benzene was used as solvent, the minor isomer accounted only for ≤ 2% of the isomer mixture, while in the more polar acetonitrile higher amounts of this adduct were isolated, with a maximum of 14% for the reaction of the **i** derivative (R^1 = 2,4,6-Me_3-3,5-Cl_2C_6; Table 3).

Table 3. Ratios (%) between the facial diastereoisomers **9** and **10** for the reactions between **1/2** (actually only isomer **1** is involved) and MTAD in C_6H_6 and CH_3CN at ca. 21 °C

Compd.[a]	R^1	R^2	C_6H_6 **9/10**	CH_3CN **9/10**
a	*t*Bu	*p*-tolyl	> 99:1[b]	> 99:1[b]
b	Ph	*p*-tolyl	> 99:1[b]	> 99:1[b]
c	Me	*p*-tolyl	98:2	89:11
d	Me	Me	> 99:1[b]	
e[c]	2,6-$Cl_2C_6H_3$	Me	94:6	88:12
f	MeCO	*p*-tolyl	98:2	95:5
g	PhCO	*p*-tolyl	98:2	
h[d]	2,4,6-$Me_3C_6H_2$	*p*-tolyl	99:1	88:12
i	2,4,6-Me_3-3,5-Cl_2C_6	*p*-tolyl	99:1	86:14
j	2,6-$Cl_2C_6H_3$	*p*-tolyl	98:2	87:13
k[e]	Ph	*p*-tolyl	>99:1[b]	

[a] Total yields > 93%. [b] Compound **10** could not be detected either by TLC or NMR analysis of the crude reaction product. [c] In CH_2Cl_2 and MeOH the **9e/10e** ratios were 91:9 and 86:14, respectively. [d] In CH_2Cl_2, **9h/10h** = 95:5. [e] From the reaction with PTAD.

We also reinvestigated the reaction between **1b/2b** (R^1 = Ph, R^2 = *p*-tolyl) and PTAD in dichloromethane. The reaction was very fast and gave high yields of a single Diels–Alder adduct, which was identical to that isolated by Saito et al. and the NMR spectroscopic data of which were very similar to those of the adduct from the corresponding reaction of **1b/2b** with MTAD. Thus, as expected, there is no difference in the reactivity of **1b/2b** with PTAD from that of the same derivative with MTAD.

As for structure assignment, Diels–Alder adducts of type **11** and **14** (Scheme 6) could be easily and safely ruled out because the high-field signals of cyclopropyl protons were absent in the ^1H NMR spectra of both the major and the minor adducts. Moreover, the NMR spectroscopic data did not reveal the presence, in either the major or the minor adducts, of a high-field vinyl proton and carbon characteristic of an enamine system, as represented by the $N^6–C^7–C^8$ moiety in **12**, nor that of two bridgehead protons coupled, with very similar *J* values, to vinyl protons ($C^1H^1–C^{15}H^{15}–C^{16}H^{16}–C^9H^9$ in **12**), and structure **12** consequently also had to be discarded.

At first sight, the ^1H NMR spectra of the isolated adducts seemed consistent with structures of type **13** as as-

signed to them by Saito et al.[5] However, there were several disturbing features that could not be reconciled with **13**. Firstly, $J_{a,c}$ (≈ 3.9 Hz) differed strongly from $J_{b,e}$ (≈ 7.0 Hz), while the rigid structure of **13** should dictate very similar dihedral angles (ca. 16° for an optimized PM3 geometry of **13d**) to the two pairs of protons involved in these couplings. Moreover, the chemical shifts of the signals attributable to C-a [at δ ($CDCl_3$) = 73−80] and C-b [at δ ($CDCl_3$) = 48−51] in **13** differed from each other by > 22 ppm, an unreasonably high difference for this type of structure. Moreover, the expected[1,2,5] typical singlet of the diheterosubstituted "spiro" carbon atom (C-g in **13**) at δ ≈ 100 was missing in the ^{13}C NMR spectra of all adducts isolated by us. Actually, the previous researchers had reported the presence of a signal at δ = 114 in the ^{13}C NMR spectra of all of the adducts [which, according to their assignment, should have structure **13** (R^3 = Ph)] isolated from reactions between PTAD and aryl-substituted compounds **1/2**. However, we were not able to detect that signal (neither for the adducts from all the reactions between MTAD and **1/2**, nor for the adduct from the reaction between **1b/2b** and PTAD), while a singlet at δ ≈ 72−79, present in the ^{13}C NMR spectra of all of the products isolated by us, was not reported by the previous authors.

Spectroscopic data (^1H NMR in Tables 4 and 5 and ^{13}C NMR in Table 6) of the adducts were fully consistent with structures **9** and **10** and were all very similar to one another, not only within the series of adducts **9** and **10**, respectively, but also if data for compounds **9** were compared with those for compounds **10**. The typical strong absorption of the CONCO system, two bands at about 1705 and 1765 cm^{-1}, was present in the IR spectra. As for ^1H NMR spectra [here exemplified by the data for adduct **9c** (R^1 = R^3 = Me; R^2 = *p*-tolyl)], the allylic proton H-6 [δ ($CDCl_3$) = 4.63] was heterocorrelated with C-6 [doublet at δ ($CDCl_3$) = 72.3] and coupled with the two vinylic protons H-7 (δ = 5.85, $J_{6,7}$ = 3.8 Hz) and H-8 (δ = 6.28, $J_{6,8}$ = 2.0 Hz) with coupling constants fully compatible with a vicinal and an allylic relationship, respectively. Interestingly, H-6 also showed a small long-range coupling with H-15 (δ = 6.19, $J_{6,15}$ = 1.2 Hz) as a result of a W (although distorted) coupling path. Proton H-8 exhibited the required *cis*-vicinal vinyl coupling to H-7 ($J_{7,8}$ = 11.2 Hz), while its coupling to H-9 [δ = 4.90, heterocorrelated with C-9 (doublet at δ = 50.2), $J_{8,9}$ = 7.1 Hz] was also completely reasonable. Proton H-9 was in turn also coupled to H-16 (δ = 6.73, $J_{9,16}$ = 7.2 Hz) and to H-15 ($J_{9,15}$ = 0.8 Hz and $J_{15,16}$ = 9.3 Hz). Other diagnostic signals supporting structure **9** (and **10**), were the singlets attributable to C-1 [at δ = 74.2 for **9c** ($CDCl_3$)] and to C-3 (at δ = 152.8 for **9c**).

The only significant difference, which was also diagnostically useful, between the ^1H NMR spectra of the minor isomers **10** and those of their counterparts **9** was the absence in the former compounds of the long-range coupling constant between H-6 and H-15, as these two protons do not have a W relationship in **10**.

Irradiation of the methyl groups at position 2 in **9e** and **10e** (R^1 = 2,6-Cl_2-C_6H_3, R^2 = Me) brought about NOE

Table 4. Representative ^1H NMR chemical shifts (δ, in $CDCl_3$) for adducts **9a−h**, **10a−h** (R^1 and R^2 as in Table 1 and 3, R^3 = Me), and **9k** (R^1 = Ph, R^2 = *p*-tolyl and R^3 = Ph)

Compd.[a]	H-6	H-7	H-8	H-9	H-15	H-16	NMe[b]
9a	4.46	5.83	6.31	4.87	6.12	6.61	3.11
9b	4.78	5.92	6.39	4.96	6.09	6.69	3.17
9c[c]	4.63	5.85	6.28	4.90	6.19	6.73	3.05
10c[c]	4.63	5.76	6.21	4.94	6.02	6.65	3.14
9e[d]	4.68	5.89	6.35	5.06	6.11	6.91	3.09
10e[d]	4.68	5.83	6.19	5.08	6.17	6.91	3.13
9f[e]	4.63	5.88	6.35	4.97	6.04	6.74	3.09
10f[f]	4.60	5.79	6.24	5.00	6.14	6.76	3.15
9h[g]	4.91	5.95	6.28	4.98	6.46	6.89	2.99
10h[h]	4.79	5.88	6.19	4.98	6.09	6.69	3.20
9k	4.92	5.98	6.47	5.07	6.12	6.72	NPh

[a] The Me group of the *p*-tolyl group absorbs at δ ≈ 2.21 in **9b**, **9h**, and **9k** and in the range δ = 2.32−2.38 in all the other compounds. [b] Me group of the triazolidinedione. [c] Me at position 3 absorbs at δ = 1.80 and 1.73 in **9c** and **10c**, respectively. [d] NMe at position 2 resonates at δ = 2.88 and 2.78 in **9e** and **10e**, respectively. [e] MeCO absorbs at δ = 2.32. [f] The CMe and MeCO signals are buried under the corresponding signals of **9f**. [g] δ = 2.11, 2.17 and 2.67 (three Me). [h] δ = 2.13, 2.21 and 2.51 (three Me).

Table 5. Representative ^1H coupling constants (*J* in Hz) for adducts **9a−h**, **10a−h** (R^1 and R^2 as in Table 1 and 3, R^3 = Me), and **9k** (R^1 = Ph, R^2 = *p*-tolyl and R^3 = Ph)

Compd.[a]	$J_{6,7}$	$J_{6,8}$	$J_{6,15}$	$J_{7,8}$	$J_{8,9}$	$J_{9,15}$	$J_{9,16}$	$J_{15,16}$
9a	3.7	2.0	1.2	11.0	7.0	1.0	7.0	9.5
9b	3.6	2.0	1.2	11.0	7.0	1.0	7.0	9.4
9c	3.8	2.0	1.2	11.2	7.1	0.8	7.2	9.3
10c	3.9	1.6	−	11.0	7.0	0.8	7.4	9.6
9e	3.8	1.8	1.1	11.1	7.0	1.1	7.1	9.1
10e	2.6	2.0	-	11.0	7.0	0.7	7.2	9.2
9f	3.7	1.9	1.2	11.0	7.0	1.0	7.0	9.3
10f	2.8	1.9	-	11.0	7.0	0.7	7.0	9.5
9h	4.0	1.8	1.2	11.1	7.0	0.5	7.2	9.2
10h	2.5	2.0	-	11.0	7.0	0.7	7.0	9.5
9k	3.7	2.1	1.4	11.2	7.0	0.8	7.0	9.5

[a] H-7 and H-9 are involved, in all compounds, in a very small coupling (*J* ≈ 0.8 Hz).

Table 6. Representative ^{13}C NMR chemical shifts (δ, in $CDCl_3$) for compounds **9** and **10**

Compd.[a]	C-1	C-3	C-6	C-7	C-8	C-9	C-15	C-16	NMe
9a	77.3	164.2	73.5	128.6	129.2	49.3	129.7	133.6	25.3
9b	75.9	157.7	73.9	128.2	129.7	49.2	129.2	134.0	25.3
9c	74.2	152.8	72.3	128.5	128.6	50.2	130.0	134.2	25.3
10c	73.5	152.1	78.2	125.8	128.7	48.0	130.2	135.4	25.3
9e	72.5	150.0	71.6	128.3	128.8	49.9	130.3	135.4	25.4
10e	76.3	153.5	79.3	128.7	127.3	48.4	126.4	136.4	25.3
9h	73.1	151.6	71.0	128.6	127.7	50.9	131.3	133.4	25.2
10h	76.2	154.7	79.6	126.4	127.5	48.8	127.6	135.3	25.6
9k	76.3	157.9	74.1	127.9	129.8	49.4	129.2	134.0	NPh

[a]C-1 and C-3 give singlets, while C-6, C-7, C-8, C-9, C-15, and C-16 give doublets, and NMe gives a quadruplet. Carbon atoms of the two carbonyl groups of the triazolidinedione moiety resonate as singlets in the δ = 150−156 range.

enhancements (by 4.5% and 12.4%, respectively) of the signals of H-15, thus confirming that the NMe group of the six-membered heterocyclic ring is close to this proton in both compounds.

Unambiguous and definitive confirmation of structures **9** was obtained by single-crystal (obtained by slow evaporation of a $CDCl_3$ solution) X-ray analysis of the hydrated adduct **9h**$-H_2O$ (Figures 2 and 3).[33] The nitrogen centers (N^{10} and N^{14}) of the triazolidinedione moiety were, as expected,[34,35] significantly pyramidal, with the five-membered ring *syn* with respect to the $C^6-C^7-C^8$ bridge (Figure 2). The dihedral angle between the triazolidine ring plane and the $C^1-N^{14}-N^{10}-C^9$ plane was 140.8°.

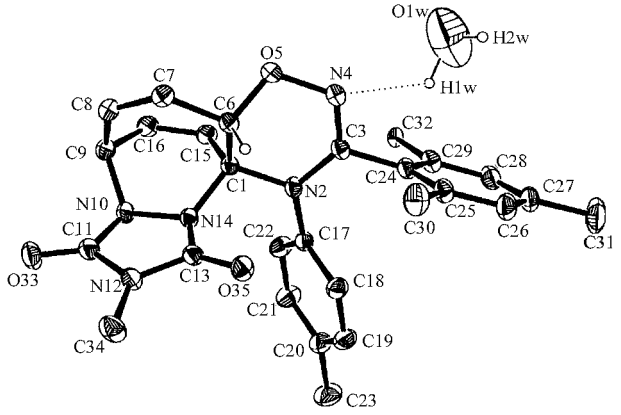

Figure 2. ORTEP plot of **9h**$-H_2O$ with atom labelling (ellipsoids at 25% probability); for clarity, only the hydrogen atom attached to C^6 has been depicted

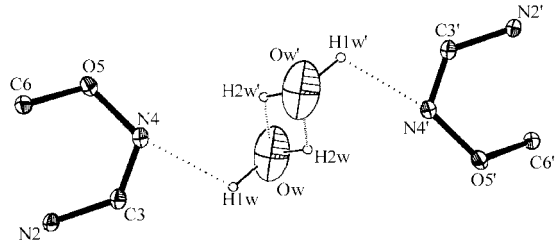

Figure 3. ORTEP plot of the water dimer that connects the two enantiomers of **9h**$-H_2O$ present in the centrosymmetric triclinic cell

The sums of the angles at N^{10} [337.2(2)°] and at N^{14} [350.1(2)°] indicated that both centers were slightly less pyramidal than in trimethylamine (333°; B3LYP/6-31G* and MM2 calculations) and that the former center was more pyramidal than the latter. This observation was also attested to by the heights of the pyramids with the nitrogen atom at the apex and the three atoms connected to it at the base [0.403(2) Å for N^{10} and 0.261(2) Å for N^{14}]. The triclinic unit cell was centrosymmetric and contained the two enantiomers of **9h**, linked to each other by a water dimer through hydrogen bonding at the N^4 centers (Figure 3). The ^1H NMR spectrum of the material of the crystal used for the X-ray analysis was equal in all respects to that of the crude major adduct **9h**.

The structures of compounds **9** and **10** in solution should look very like that shown in Figure 2, in particular as far as conformational choice between invertomers at the nitrogen centers (N^{10} and N^{14}) is concerned. In fact, geometry optimization with the PM3 method revealed that the more stable invertomers of compounds **9** and **10** exhibited the same structure as that in the solid state **9h**$-H_2O$.

To conclude, reactions between nitrile oxide−azaheptafulvene adducts (i.e., **1/2**) and TADs are always fast and very clean and involve only the fused isomer **1** no matter towards which side the **1/2** equilibrium is shifted. They exhibit complete regioselectivity (only the $C^{4a}-C^5-C^6-C^7$ diene moiety of **1** is involved) and high facial selectivity (with strongly dominant attack on the top face of **1**, *syn* to the hydrogen atom at position 9a). The position of the equilibrium is certainly reflected, to some extent, in the reaction rate; competition experiments (in benzene) demonstrated that **1a/2a** (**1a/2a** < 1:99) reacts eight times more slowly than **1c/2c** (**1c/2c** = 70:30).

Some Mechanistic Considerations

Literature data (some results are reported in Scheme 5) clearly indicate that there are examples of formal Diels−Alder cycloadditions of TADs involving either only the cycloheptatriene form or only the norcaradiene isomer, in systems in which only the former isomer can be detected by spectroscopic techniques. The reaction outcome obviously reflects both the energy difference between the rapidly equilibrating valence tautomers and the activation energy difference of their reaction with TAD. The computational data in Schemes 3 and 4 and the experimental data in Scheme 5 demonstrate that the norcaradiene isomer, owing to its intrinsic high reactivity with TAD, can favorably counteract a large (more than 5 kcal/mol) ground state energy gap with respect to its cycloheptatriene counterpart (as in the case of **3a**, **3e**, and a derivative of **4**, that is, **7**). However, when the bicyclic isomer is considerably less stable than the monocyclic isomer (i.e., by more than 10 kcal/mol) the latter enters into cycloaddition in preference of the former, as shown by the reactions between **3b** and **3d** and PTAD (Scheme 5).

Thus, the absence of Diels−Alder-type adducts derived from **1***ncd* and **2***ncd* in the reaction between nitrile oxide−azaheptafulvene adducts and TAD can mostly be attributed to the high energy of these isomers (≥ 13 kcal/mol higher than the corresponding triene derivatives, Scheme 2).

As for competition between the "fused" **1***cht* and "spiro" **2***cht* cycloheptatriene isomers, it is noteworthy that compound **a**, which on the basis of NMR spectroscopic data exists only (Table 1) in the "spiro" form **2a***cht*, affords products derived only from the "fused" cycloheptatriene form **1a***cht*. Attempts to document the presence of norcaradiene isomers by using MTAD failed but, as a by-product, this allowed us to demonstrate that the "spiro"/"fused" isomer equilibrium is actually operative for all of the nitrile oxide−azaheptafulvene adducts even when only one isomer is detectable by spectroscopic techniques.

This finding also demonstrates that the activation energy of the reaction between **1a***cht* with MTAD is lower than that of its **2a***cht* counterpart by > 5 kcal/mol and suggests that the difference in reactivity between the **1***cht* and **2***cht* forms in favor of the former is large for all of the nitrile oxide−azaheptafulvene adducts.

Triazolinediones are among the most reactive dienophiles known and have strong electrophilic character.[36−38] Consequently, their higher reactivity with **1***cht* than with **2***cht* strongly suggests that the polyene system of the former is more electron-rich than that of the latter. However, in order to convincingly explain the higher reactivity of **1***cht* relative to **2***cht* and the facial selectivity observed for **1***cht*, one must confidently know the reaction mechanism. And this is not the case for TAD reaction with dienes.

Recent DFT calculations by Houk et al.[39] on the reaction between the parent triazolinedione (R^3 = H) and butadiene demonstrated that the TS of the concerted (e.g., **15**; Scheme 7) Diels−Alder-type attack is highly asynchronous and ca. 3−6 kcal/mol lower in energy (gas phase) than the TS giving rise to aziridinium imide (AI, e.g. **16**) intermediates. These authors were not able to locate an AI on the pathway to adducts in the case of the *s-cis*-butadiene reaction, but they stated that "for substituted dienes ... the energetics of a stepwise mechanism via AI intermediates would be even more favorable than for butadiene".

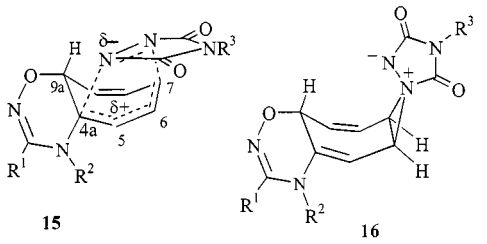

Scheme 7

That is, it is not possible to choose definitely between a concerted and stepwise mechanism for the reaction between cycloheptatrienes and TADs and this problem must be addressed by locating transition structures with good-level calculations, possibly with inclusion of solvent effects. We are now undertaking such a study.

Conclusions

The nitrile oxide−azaheptafulvene adducts consist of mixtures of rapidly equilibrating fused (**1***cht*) and spiro (**2***cht*) cycloheptatriene isomers, the ratios of which can be evaluated by ^{1}H NMR and correctly predicted by B3LYP/6-31G* calculations. The norcaradiene isomers (**1***ncd*) and (**2***ncd*), undetectable by spectroscopic methods, are predicted by calculations to be much less stable (by ≥ 13 kcal/mol) than the cycloheptatriene isomers and they do not actually compete with them in intermolecular reactions. The nitrile oxide−azaheptafulvene adducts enter into a very fast reaction with triazolinediones to afford two facial adducts, **9** (strongly dominant) and **10**, both derived from TAD attack on the enaminic diene system of the fused form (**1***cht*) even when this form is not detectable by NMR spectroscopy. Our results revise the previous wrong structure assignment to these adducts, which were described as deriving from **2***cht*.

Experimental Section

General Remarks: Melting points are uncorrected and were measured with a Büchi 535 apparatus. Elemental analyses were performed with a Carlo Erba CHN analyzer, model 1106. IR spectra were recorded either as Nujol suspensions or as films, with a Perkin−Elmer 881 spectrophotometer. ^{1}H and ^{13}C NMR spectra were recorded with a Bruker AE 300 spectrometer (operating at 300.3 and 75.5 MHz, respectively) with tetramethylsilane as internal standard at 20° C for $CDCl_3$ solutions (unless otherwise stated). Protons were correlated by decoupling and COSY experiments, while carbon atoms were correlated to protons by ^{1}H-^{13}C heterocorrelated spectra. ^{1}H NMR spectra were analyzed as first-order spectra. Thin layer chromatograms were performed on plates precoated with 60 GF_{254} silica gel (Merck). Spots were viewed either by spraying with 3% chromic oxide in sulfuric acid (50%) followed by heating at 120 °C or under UV light. Column chromatography was performed with 60 silica gel (70−230 mesh) Merck. MTAD and PTAD[40] were purified by sublimation before use.

General Procedure for Reactions between TADs and 1/2: A solution of freshly sublimed MTAD or PTAD (0.40 mmol, 46 mg for MTAD and 70 mg for PTAD)[40] in anhydrous benzene (5 mL) was added dropwise to a solution of freshly purified **1/2**[1,2] (0.40 mmol) [**a**, 118 mg; **b**, 126 mg; **c**, 101 mg; **d**, 71 mg; **e**, 123 mg; **f**, 112 mg; **g**, 137 mg; **h**, 143 mg; **i**, 170 mg; **j**, 153 mg] in anhydrous benzene (5 mL). The reaction was allowed to proceed at room temperature (20−23 °C) whilst stirring. The red-violet color of MTAD faded rapidly (from a few seconds to some minutes), leaving a colorless solution with a colorless precipitate. TLC analysis (eluent: ethyl acetate/benzene/dichloromethane = 40:40:20) of the crude reaction mixture revealed the complete disappearance of **1/2** and the presence (as a rule) of two adducts, with the minor component exhibiting a lower R_f than the major one. The reaction mixture was left at room temperature for 15 min and the solvent was evaporated under reduced pressure to afford an almost quantitative yield of a colorless solid. The isomer ratio was evaluated by ^{1}H NMR analysis of the crude product and the two isomers were separated by column chromatography, eluting with a benzene/ethyl acetate/dichloromethane (40:40:20) mixture. The products obtained by chromatography [**9a**, 153 mg (94%); **9b**, 164 mg (96%); **9c**, 139 mg (95%); **10c**, 3 mg (2%); **9d**, 108 mg (93%); **9e**, 155 mg (92%); **10e**, 10 mg (6%); **9f**, 145 mg (92%); **10f**, 3 mg (2%); **9g**, 166 mg (91%); **10g**, 3 mg (1.5%); **9h**, 176 mg (94%); **10h**, 2 mg (1%); **9i**, 200 mg (93%); **10i**, 2 mg (1%); **9j**, 181 mg (91%); **10j**, 4 mg (2%); **9k**, 183 mg (93%)] proved to be homogeneous by ^{1}H NMR analysis and were used as such for elemental analysis. Further purification was achieved by crystallization from benzene in the case of **9a** and from ethyl acetate or ethyl acetate/dichloromethane for other adducts. All of the adducts produced colorless crystals that melted with decomposition. The reaction was also carried out in acetonitrile under otherwise similar conditions and the color disappearance seemed to be slightly slower than in benzene. The results were similar to those obtained in benzene and the only significant difference was a decrease in the **9/10** ratio. The IR spectra of all compounds

9 and **10** displayed two bands at about 1765 (m) and 1705 (vs) cm^{-1}, attributable to the CONRCO group. The NMR spectroscopic data of several adducts are reported in Tables 4−6.The ^{1}HNMR spectra of **9d**, **9g**, **10g**, **9i**, **10i**, **9j**, and **10j** and the ^{13}C NMR spectra of **9d** and **9j** are similar in all respects to the spectra collected in Tables 4−6.

Compound 9a: M.p. 198 °C with decomposition. $C_{22}H_{25}N_5O_3$ (407.5): calcd. C 64.85, H 6.18, N 17.19; found C 65.08, 6.31, N 16.96.

Compound 9b: M.p. 181 °C with decomposition. $C_{24}H_{21}N_5O_3$ (427.5): calcd. C 67.43, H 4.95, N 16.39; found C 67.18, H 4.82, N 16.22.

Compound 9c: M.p. 186 °C with decomposition. $C_{19}H_{19}N_5O_3$ (365.4): calcd. C 62.45, H 5.24, N 19.17; found C 62.40, H 5.47, N 19.06.

Compound 10c: Glassy solid. $C_{19}H_{19}N_5O_3$ (365.4): calcd. C 62.45, H 5.24, N 19.17; found C 62.31, H 5.43, N 19.02.

Compound 9d, M.p. 170 °C with decomposition. $C_{13}H_{15}N_5O_3$ (289.3): calcd. C 53.97, H 5.23, N 24.21; found C 53.75, H 5.32, N 24.04.

Compound 9e: M.p. 201 °C with decomposition. $C_{18}H_{15}Cl_2N_5O_3$ (420.3): calcd. C 51.44, H 3.60, N 16.66; found C 51.33, H 3.45, N 16.57.

Compound 10e: M.p. 197 °C with decomposition. $C_{18}H_{15}Cl_2N_5O_3$ (420.3): calcd. C 51.44, H 3.60, N 16.66; found C 51.42, H 3.56, N 16.58.

Compound 9f: M.p. 205 °C with decomposition. $C_{20}H_{19}N_5O_4$ (393.4): calcd. C 61.06, H 4.87, N 17.80; found C 60.86, H 4.87, N 17.67.

Compound 10f: This was not isolated but its presence was reliably detected by ^{1}HNMR spectroscopy (see Tables 4 and 5).

Compound 9g: M.p. 185 °C with decomposition. $C_{25}H_{21}N_5O_4$ (455.5): calcd. C 65.92, H 4.65, N 15.38; found C 65.88, H 4.79, N 15.29.

Compound 10g: This was not isolated but its presence was detected by ^{1}HNMR analysis.

Compound 9h: Colorless powder from ethyl acetate. M.p. 170 °C with decomposition. $C_{27}H_{27}N_5O_3$ (469.5): calcd. C 69.06, H 5.80, N 14.92; found C 68.88, H 5.95, N 14.81.

Compound 10h: Glassy solid. $C_{27}H_{27}N_5O_3$ (469.5): calcd. C 69.06, H 5.80, N 14.92; found C 69.07, H 5.91, N 14.98.

Compound 9i: M.p. 195 °C with decomposition. $C_{27}H_{25}Cl_2N_5O_3$ (538.4): calcd. C 60.23, H 4.68, N 13.01; found C 60.38, H 4.55, N 13.01.

Compound 10i: M.p. 177 °C with decomposition. $C_{27}H_{25}Cl_2N_5O_3$ (538.4): calcd. C 60.23, H 4.68, N 13.01; found C 60.03, H 4.84, N 12.86.

Compound 9j: M.p. 169 °C with decomposition. $C_{24}H_{19}Cl_2N_5O_3$ (496.4): calcd. C 58.07, H 3.86, N 14.11; found C 57.97, H 3.94, N 14.10.

Compound 10j: M.p. 163 °C with decomposition. $C_{24}H_{19}Cl_2N_5O_3$ (496.4): calcd. C 58.07, H 3.86, N 14.11; found C 57.93, H 3.91, N 13.98.

Compound 9k: From the reaction between **1b/2b** and PTAD. M.p. 209 °C with decomposition (ref.[5] 210−212 °C with decomposition). $C_{29}H_{23}N_5O_3$ (489.5): calcd. C 71.15, H 4.74, N 14.31; found C 70.92, H 4.85, N 14.21.

Competition Reactions: A solution of MTAD (38 mg, 0.34 mmol) in benzene (5 mL) was added dropwise with stirring at 21 °C to a solution of **1a/2a** (166 mg, 0.56 mmol) and **1c/2c** (132 mg, 0.36 mmol) in anhydrous benzene (10 mL). Color disappearance took place at once. After 15 min at room temperature, the solvent was evaporated and the crude residue was analyzed by ^{1}H NMR to determine the ratio between adducts **9a** and **9c** (16:84). The rate constant ratio for compounds **a** and **c** (k_c/k_a = 7.8) was evaluated according to Huisgen et al.[41] on the basis of the reasonable assumption of a quantitative yield of adducts. The competition reaction was repeated by using similar amounts of reactants to give k_c/k_a = 8.5. A similar reaction was also carried out for **1c/2c** (100 mg, 0.27 mmol) in competition with **1j/2j** (150 mg, 0.30 mmol) toward MTAD (31 mg), under the same conditions as described above, to give a **9c/9j** ratio of 83:17 (^{1}H NMR analysis). The obtained rate constant ratio (5.1) was substantially confirmed in a second experiment (4.6) and indicated a rate-retarding effect by the 2,6-Cl_2-C_6H_3 group with respect to the methyl group.

Computational Methods: The geometry optimizations for all the stationary points were performed by use of the hybrid density functional B3LYP method, as implemented in the TITAN (version 1.0.5) suite of programs, using the 6−31G* basis set. Several minima were also optimized with *Gaussian 94*.[42] The results obtained by the two packages of programs were consistent with each other. The data reported here are those obtained with Titan programs. The harmonic vibrational frequencies were also calculated for all stationary points to identify transition structures (one imaginary frequency) and minima (all positive frequencies) and were used unscaled[43] to obtain zero point vibrational energies (ZPEs) as well as contributions of molecular motion to the enthalpy and free energy for T = 298.15 K. In most cases the total energy was also evaluated by single-point calculations with a larger basis set (B3LYP/6-311+G**//B3LYP/6-31G*) at the lower level geometries. Titan [*Gaussian 94*] absolute B3LYP/6-31G* energies (Hartree) + VZPE (Hartree) for some stationary points are as follows: **1***cht*, −572.908980 + 0.206805; (o)-**2***cht*, −572.905310 [−572.905476] + 0.205135; **3a***cht*, −271.509448 [−271.509593] + 0.128444; **3b***cht*, −469.987030 [−469.987192] + 0.112565; **3c***cht*, −455.966127 [−455.965948} + 0.124699; **3d***cht*, −499.349990 [−499.349752] + 0.172826; **3e***cht*, −538.665437 [−538.665621] + 0.202371; **4***cht*, −387.015767 + 0.168592. In the case of compounds **3e**, the energies refer to the most stable conformer as far as the six-membered ring is concerned (i.e., the chair conformer). The most stable conformation of the dioxolane ring of compounds **3d** is a twist-like conformation (with the spiro carbon atom and the two oxygen atoms in a plane and the other two carbon atoms out of plane; an envelope conformation is 1.0 kcal/mol higher in energy) while in the case of derivatives **3e** the trioxolane ring adopts a distorted envelope conformation (with the distal oxygen atom of the peroxy system as the out-of-plane atom). A relatively flat envelope conformation, with the spiro carbon atom as the out-of-plane atom, is also exhibited by the oxadiazoline ring in compounds **2**. The heterocyclic six-membered ring of **1***cht* is conformationally flexible and we located two conformations **1***cht* and **1**′*cht*. The second one, **1**′*cht*, resides at a slightly higher energy (Titan, −572.905866 Hartree; Gaussian, −572.905970 Hartree) than the former one (see above). Animation of vibrations showed that those corresponding to planarization of the seven-membered ring have low frequencies:

(o)-**2***cht*, ν = 65 cm^{-1}, **3a***cht*, ν = 216 cm^{-1}; **3b***cht*, ν = 75 cm^{-1}, **3c***cht*, ν = 102 cm^{-1}, **3d***cht*, ν = 64 cm^{-1}, **3e***cht*, ν = 94 cm^{-1}. The imaginary frequencies for the ring inversion TSs are very low (**3a***cht*, ν_i = −93 cm^{-1}; **3b***cht*, ν_i = −45 cm^{-1}; **3c***cht*, ν_i = −32 cm^{-1}; **3d***cht*, ν_i = −23 cm^{-1}; **3e***cht*, ν_i = −16 cm^{-1}) while those for TSs$_{cht,ncd}$ are about −400 cm^{-1} (**1d**, −337 cm^{-1}; (o)-**2d**, −406 cm^{-1}; **3a**, ν_i = −435 cm^{-1}; **3b**, ν_i = −359 cm^{-1}; **3c,** ν_i = −465 cm^{-1}; **3d**, ν_i = −395 cm^{-1}; **3e**, ν_i = −406 cm^{-1}; **4**, ν_i = −412 cm^{-1}). Absolute energies, geometry data, and Cartesian coordinates for all stationary points are available on request.

X-ray Crystallographic Study: The crystals were colorless prisms obtained by crystallization induced by slow concentration of a chloroform solution of **9h.** ORTEP[44] views of the molecular structure of **9h**−H_2O and the numbering scheme are shown in Figures 2 and 3. Accurate unit cell parameters were obtained from least-squares fit of 2θ values for 25 reflections; the triclinic nature of the unit cell was confirmed by use of the TRACER program.[45] The structure was solved by direct methods and the *E* map correctly found all non-hydrogen atoms in the molecule. The hydrogen atoms were located by a three-dimensional difference Fourier synthesis and compared with those calculated from the geometry of the molecule, and refined isotropically in the subsequent least-squares cycles. In all refinement stages the observed reflections were given unit weight, since the use of weights obtained from counting statistics did not give better results. A summary of crystal data, data collection, and structure refinement is given in Table 7.[46]

Table 7. Crystal data, data collection, and structure refinement for **9h**−H_2O

Empirical formula	$C_{27}H_{29}N_5O_4$
Color/shape	colorless/prisms
Molecular mass	487.6
Temperature	293 K
Crystal system	triclinic
Space group	$P\bar{1}$
a [Å]	10.847(2)
b [Å]	12.551(1)
c [Å]	10.750(2)
α [°]	91.46(1)
β [°]	110.36(1)
γ [°]	89.11(1)
V [Å^3]	1371.7(4)
Z	2
$D_{calcd.}$ [g·cm^{-3}]	1.18
μ [cm^{-1}]	6.7
Diffractometer, scan	Enraf−Nonius CAD-4, ω/2θ
Radiation/wave length	Cu-K_α (graphite monochrom.)/1.5418 Å
F(000)	516
Crystal size	0.77 × 0.49 × 0.42 mm
Range for data collect. [°]	2 ≤ θ ≤ 35°
Index ranges	$0 \le h \le 13$, $-15 \le k \le 15$, $-13 \le l \le 13$
Reflections collected	5183
Independent/observed refls.	4591 [R_{int} = 0.014)/4182 ($I \ge 2\ \sigma\ (I)$]
Corrections applied	Lorentz polarization
Absorption factors[47]	0.9785, 0.9995
Refinement method	Full-matrix, least-squares on F^2
Computing[48]	Enraf−Nonius SDP
Parameters varied	441
Goodness-of-fit on F^2 [a]	0.680
Weights	σ^{-2} ($\|F_o\|$)
Final *R* indexes	R[b] = 0.041, Rw[c] = 0.057
Largest diff.peak/hole [e/Å^3]	Δρ = 0.559/−0.183

[a] $GOF = [w(k^{-1}\|F_o\| - \|F_c\|)^2/(N_o - N_v)^{1/2}$; N_o = 4182, N_v = 441. [b] $R = (\|F_o\| - k\|F_c\|)/\|F_o\|$. [c] $Rw = [w(\|F_o\| - k\|F_c\|)^2/w|F_o|^2]^{1/2}$.

Acknowledgments

The authors thank the M. U. R. S. T. (Ministero dell'Università e della Ricerca Scientifica e Tecnologica, Italy) and the CNR for financial support.

[1] R. Gandolfi, A. Gamba, P. Grünanger, *Heterocycles* **1995**, *40*, 619−638.
[2] M. Freccero, R. Gandolfi, M. Sarzi-Amadé, *Heterocycles* **1998**, *47*, 453−468.
[3] The descriptor *cht* is used for all of the compounds exhibiting a cycloheptatriene ring while their norcaradiene isomers are labeled with the descriptor *ncd.* The descriptors (i) and (o) indicate the two isomers of the boat structure for 7,7-disubstituted (with different substituents) cycloheptatriene derivatives according to whether the higher CIP priority atom (of the two atoms directly attached at position 7) is inside or outside, respectively.
[4] K. Ito, K. Saito, K. Takahashi, *Heterocycles* **1993**, *36*, 21−24.
[5] K. Ito, K. Saito, *Bull. Chem. Soc. Jpn.* **1995**, *68*, 3539−3547.
[6] G. Maier, *Angew. Chem. Int. Ed. Engl.* **1967**, *79*, 402−413.
[7] J. F. Liebman, A. Greenberg, *Chem. Rev.* **1989**, *89*, 1225−1246.
[8] For references on Diels−Alder reactions of cycloheptatriene derivatives: F. Fringuelli. A. Taticchi, *Dienes in the Diels−Alder reaction*, Wiley-Interscience, New York, **1990**, pp. 232−234.
[9] G. Welt, E. Wolf, P. Fischer, B. Föhslich, *Chem. Ber.* **1982**, *115*, 3427−3435.
[10] T. Knoechel, W. Pickl, J. Daub, *J. Chem. Soc., Chem. Commun.* **1982**, 337−338.
[11] W. Adam, M. Balci, B. Pietrzak, *J. Am. Chem. Soc.* **1979**, *101*, 6285−6294.
[12] W. Adam, H. Rebollo, H. Bürr, K.-H. Pauly, *Tetrahedron Lett.* **1982**, *23*, 923−926.
[13] For sake of simplicity only one of the two possible facial attacks of MTAD on **1***cht*, **1***ncd*, **2***cht*, and **2***ncd* to give **11**−**14** is depicted in Scheme 6.
[14] While the reversible **1/2** isomerization (through a dipolar ion exhibiting a tropylium moiety; Scheme 2) takes place readily at room temperature, related isomerizations (e.g., that from spiro compound **3d***cht* to a fused form or from 7,7-dimethoxycycloheptatriene to 1,7-dimethoxy derivative occur smoothly only on heating (e.g., at > 70 °C).[15−17] In the case of dialkylthiocycloheptatrienes, isomerization is fast, but only the 1,7-derivative could be detected.[18,19] As a rule, the 1,7-derivatives seem to be thermodynamically favored over their 7,7-counterparts.
[15] T. Fukunaga, *Tetrahedron Lett.* **1970**, 2975−2978.
[16] R. W. Hoffmann, K. R. Eichev, H. J. Luthardt, B. Dittrich, *Chem. Ber.* **1970**, *103*, 1547−1560.
[17] D. Mukherjee, L. N. Domelsmith, K. N. Houk, *J. Am. Chem. Soc.* **1978**, *100*, 1954−1957.
[18] M. Cavazza, G. Morganti, F. Pietra, *J. Chem. Soc., Chem. Commun.* **1978**, 945−946.
[19] M. Cavazza, G. Morganti, F. Pietra, *Tetrahedron Lett.* **1978**, 2137−2138.
[20] T. Ting-Hua, C. S. Q. Lew, Y.-P. Cui, B. Capon, I. G. Csimadia, *J. Mol. Struct. (Theochem)* **1994**, *305*, 149−164 and references cited therein.
[21] A. A. Jarzecki, J. Gajewski, E. R. Davidson, *J. Am. Chem. Soc.* **1999**, *121*, 6928−6935.
[22] For a very recent investigation of the conformational equilibrium of 1,3,5-cycloheptatriene-7-d by ^{1}H NMR spectroscopy and ab initio calculations [RHF/6-31G*, MP2/6-31G* and MP4/6-31G* (single point)], see: D. I. Freedberg, M. Kopelevich, F. A. L. Anet, *J. Phys. Org. Chem.* **2001**, *14*, 625−635.
[23] C. Berger, S. Dietrich, U. Dilger, D. Geuenich, H. Helios, R. Herges, P. Kirchmer, H. Röttele, G. Schröder, *Angew. Chem. Int. Ed.* **1998**, *37*, 1854−1857.
[24] The absolute energies for (o)-**3f***cht* and (i)-**3f***cht* obtained by *Gaussian 94* [TITAN values in brackets] programs are as fol-

lows: (o)-**3f***cht* −535.175861 Hartree {α = 8.5°, β = 3.3° and γ = 4.5°} (ref. −535.17585 Hartree)[23] [−535.175917 Hartree] and (i)-**3f***cht* 535.175308 Hartree {α = 36.5°, β = 15.5° and γ = 19.5°} [−535.175169 Hartree]. Two minima, corresponding to (o)-**3f***cht* and (i)-**3f***cht*, were also located at the HF/6-31G* level [with TITAN programs]. The out-of-plane distortion is high in both conformers [(o)-**3f***cht*: α = 38.5°, β = 19.1° and γ = 24.1°; (i)-**3f***cht*: α = 40.9°, β = 20.3° and γ = 25.3°)] but the planarization energy is once again small [$E_{rel.}$ = 0.3, 0.0 and 0.6 kcal/mol for (o)-**3f***cht*, (i)-**3f***cht* and the planar (constrained) form, respectively].

[25] However, there is no convincing evidence for this effect as far as bond lengths and net charge distribution are concerned.

[26] Structure (i)-**2d***cht* is also not a minimum at the HF/6-31G* level when optimization is performed with *Gaussian 94*, but a minimum corresponding to this structure (α = 34.5°, β = 16.8°, and γ = 21.0°) was located with TITAN (2.9 kcal/mol higher than (o)-**2d***cht*). An energy minimum for the inside conformation was also located with the PM3, AM1, and HF/3−21G methods. The net atomic charges (B3LYP/6-31G*) for (o)-**2d***cht* are as follows: NMe, 0.12e (CHELPG), 0.17e (Mulliken) and 0.20e (NPA), O −0.33e (CHELPG), −0.47e (Mulliken) and −0.44e (NPA). In **3d***cht* the net negative charge on the inside oxygen [−0.47e (CHELPG), −0.49e (Mulliken) and −0.58e (NPA)] is slightly lower than that on the outside one [−0.54e (CHELPG), −0.53e (Mulliken) and −0.59e (NPA)], as a reflection of the electrostatic repulsion between the inside oxygen and the π system. Note how, at the B3LYP/6-31G* level, steric effects in (o)-**2d***ncd* are almost exactly counteracted by electrostatic effects in (i)-**2d***ncd*, with resultant very similar energies for these two compounds.

[27] The only known B3LYP/6-31G* data for cycloheptatriene derivatives (for ab initio HF and post-HF data see references 20 and 22) are, as far as we know, the potential energies reported by Gajewski et al. for the isomerization processes involving the parent cycloheptatriene/norcaradiene system.[21] Our results confirm their data. Cycloheptatriene/norcaradiene isomerizations of the parent system and 7,7-difluoro and 7,7-dicyano derivatives have also already been studied at the HF/6-31G* level.[20] Potential energies (kcal/mol) for the four stationary points $TS_{inversion}$/cycloheptatriene/$TS_{cht,ncd}$/norcaradiene are as follows: 4.2 (1.2) [4.3] {1.2}, 0.0 (0.0) [0.0] {0.0}, 18.2 (22.5) [17.2] {20.1}, 5.9 (14.7) [−3.0] {10.9} for the parent system, (7,7-difluoro derivatives), [7,7-dicyano derivatives] and {7,7-ethylenedioxy derivatives}. HF/6-31G* calculations (data for all $TSs_{inversion}$ and for 7,7-ethylenedioxy derivatives are from our laboratory, while for other data see ref.[20]) considerably overestimate the energy barrier for the *cht*/*ncd* interconversion. Enthalpies from AM1 and PM3 calculations do not compare acceptably with known experimental data and with ab initio results.

[28] Computational data are gas-phase data. However, solvent effects should not heavily influence isomer equilibrium, in particular in the case of low polarity solvents such as benzene, as dipole moments of isomers of nitrile oxide−azaheptafulvene adducts are similar to each other [e.g., dipole moments are as follows: **1d***cht*, μ = 4.31 D; **1d***ncd*, μ = 4.04 D; (o)-**2d***cht*, μ = 4.51 D; (o)-**2d***ncd*, μ = 3.27 D; (i)-**2d***ncd*, μ = 4.41 D].

[29] R. Huisgen, *Angew. Chem. Int. Ed. Engl.* **1970**, *9*, 751−762.

[30] E. Giganek, *J. Am. Chem. Soc.* **1966**, *89*, 1454−1458.

[31] J. B. Lambert, L. J. Durham, P. Lepoutere, J. D. Roberts, *J. Am. Chem. Soc.* **1965**, *87*, 3896−3899.

[32] M. B. Rubin, *J. Am. Chem. Soc.* **1981**, *103*, 7791−7792.

[33] Actually, the X-ray structure for **9h** of Figure 2 is the enantiomer of structure **9** used (for sake of clarity) in Scheme 6.

[34] I. Agmon, M. Kaftory, S. F. Nelsen, S. C. Blacckstock, *J. Am. Chem. Soc.* **1986**, *108*, 4477−4484.

[35] S. F. Nelsen, P. A. Petillo, H. Chang, T. B. Frigo, D. A. Dougherty, M. Kaftory, *J. Org. Chem.* **1991**, *56*, 613−618.

[36] C. J. Moody, *Adv. Heterocycl. Chem.* **1982**, *30*, 1−45 and references therein.

[37] F. Jensen, C. S. Foote, *J. Am. Chem. Soc.* **1987**, *109*, 6376−6385.

[38] E. L. Clennan, A. D. Earlywine, *J. Am. Chem. Soc.* **1987**, *109*, 7104−7110.

[39] J. S. Chen, K. N. Houk, C. S. Foote, *J. Am. Chem. Soc.* **1998**, *120*, 12303−12309.

[40] R. C. Cookson, S. S. Gupta, I. D. R. Stevens, C. T. Watts, *Org. Synth.* **1971**, *51*, 121−

[41] K. Bast, M. Christl, R. Huisgen, W. Mack, *Chem. Ber.* **1973**, *106*, 3312−3344.

[42] M. J. Frisch, G. W. Trucks, H. B. Schlegel, P. M. W. Gill, B. G. Johnson, M. A. Robb, J. R. Cheesman, T. Keith, G. A. Petersson, J. A. Montgomery, K. Raghavachari, M. A. Al-Laham, V. G. Zakrewski, J. V. Ortiz, J. B. Foresman, J. Cioslowski, B. B. Stefanov, A. Nanayakkara, M. Challacombe, C. Y. Peng, P. Y. Ayala, W. Chen, M. W. Wong, J. L. Andres, E. S. Replogle, R. Gomperts, R. L. Martin, D. J. Fox, J. S. Binkley, D. J. Defrees, J. Baker, J. P. Stewart, M. Head-Gordon, C. Gonzales, J. A. Pople, *Gaussian 94*, Gaussian, Inc., Pittsburgh, PA, **1995**.

[43] A. Rastelli, M. Bagatti, R. Gandolfi, *J. Am. Chem. Soc.* **1995**, *117*, 4965−4975.

[44] C. K. Johnson, *ORTEP Report ORNL-3793* Oak Ridge National Laboratory, TN, **1965**.

[45] S. L. Lawton, R. A. Jacobson, TRACER, *A Cell Reduction Program*, Ames Laboratory, Iowa State University of Sciences and Technology: Ames, IA, **1965**.

[46] Crystallographic data (excluding structure factors) for the structure included in this paper have been deposited with the Cambridge Crystallographic Data Centre as supplementary publication no. CCDC-168348. Copies of the data can be obtained free of charge on application to CCDC, 12 Union Road, Cambridge CB2 1EZ [Fax: (internat.) + 44-1223/336-033; E-mail: deposit@ccdc.cam.ac.uk].

[47] A. C. I. North, D. C. Phillips, F. Scott Mathews, *Acta Crystallogr., Sect. A* **1968**, *24*, 351.

[48] B. A. Frenz, and Associates, Inc., College Station, TX 77840 and Enraf−Nonius, Delft, **1985**.

Received August 8, 2001
[O01413]